

Theoretical investigation of tautomerism in N-hydroxy amidines

Hossein Tavakol · Sattar Arshadi

Received: 28 April 2008 / Accepted: 6 December 2008 / Published online: 6 January 2009
© Springer-Verlag 2008

Abstract A DFT study with QST3 approach method is used to calculate kinetic, thermodynamic, spectral and structural data of tautomers and transition state structures of some N-hydroxy amidines. All tautomers and transition states are optimized at the B3LYP/6-311++g** and B3LYP/aug-cc-pvtz level, with good agreement in energetic result with energies obtained from CBS-QB3, a complete basis set composite energy method. The result shows that the tautomer **a** (amide oxime) is more stable than the tautomer **b** (imino hydroxylamine) as is reported in the literature. In addition, our finding shows that, the energy difference between two tautomers is only in about 4–10 kcal/mol but the barrier energy found in traversing each tautomer to another one is in the range of 33–71 kcal/mol. Therefore, it is impossible to convert these two tautomers to each other at room temperature. Additionally, transition state theory is applied to estimate the barrier energy and reaction rate constants of the hydrogen exchange between tautomers in presence of 1–3 molecules of water. The computed activation barrier shows us that the barrier energy of solvent assisted tautomerism is about 9–20 kcal/mol and lower than simple tautomerism and this water-assisted tautomerism is much faster than simple tautomerism, especially with the assisting two molecules of water.

Keywords DFT calculations · N-hydroxy amidines · Tautomers · Transition state

H. Tavakol (✉)
Chemistry Department, Science Faculty, University of Zabol,
Zabol, Iran
e-mail: h_tavakol@uoz.ac.ir

S. Arshadi
Chemistry Department, Science Faculty,
University of Payame Noor,
Tehran, (Behshahr Unit), Iran

Introduction

In the course of a recent study on the tautomerism of organic compounds, we focused our research on amidoximes or N-hydroxy amidines. N-hydroxy amidines are versatile precursors of many heterocyclic compounds of pharmaceutical importance [1, 2]. In addition, it inhibits platelet aggregation [3] and induces vasorelaxation in rat aorta [4, 5].

This group is not only used in synthesis of various organic and useful compounds [6–9], specially such as heterocycles [10, 11], polymeric nano fibers [12, 13] and new polymers [14–16], but also it can be applied in drug synthesis and biologic materials [17–19], trace analysis membrane [20], extraction of heavy metals such as Uranium and Cadmium [21–25] and new peptide synthesis [26]. Also, these compounds can be used in treatment of some hazardous disease such as AIDS [27, 28] and malaria [29].

Another interesting aspect of N-hydroxy amidines is existence of two probable tautomeric forms, one is amide oxime (with -NH-C=N-O- structure) and the other is imino hydroxylamine (with -N=C-NH-O- structure). In all reported experiments related to N-hydroxy amidines, only tautomer **a** was observed and it is a major tautomer [11, 17, 20, 30–32]. It is clear that study of these two tautomers and the way they are conversed, not only expands our knowledge about tautomerism, but also it leads us to be able to learn more about N-hydroxy amidines.

The importance of tautomerism is revealed since in recent years the investigation about tautomerism has been one of the major topics in theoretical chemistry. By reviewing the literature, many papers about study of tautomerism have been found. Among these, we can find some papers about tautomerism in carbon-carbon [33], keto-enol [34], imine-enamine [35], amide-iminol [36], and thioamide-iminothiole systems [37], and some other papers

about study of tautomerism in DNA bases [38] and other natural product [39].

To our best knowledge, a literature survey of N-hydroxy amidines showed us no papers about theoretical study of tautomerism in N-hydroxy amidines. Thus, computational methods have become increasingly important in the determination of accurate properties of compounds, so, we decided to do some computational investigations about these compounds to calculate important properties of their tautomers and transition states in gas phase and ground state.

These compounds can be prepared easily and some different methods in preparing them are reported in the literature [30–32].

Methods

Density functional theory (DFT) has been widely applied by physicists to study the electronic structure of solids in the past 30 years [40–48]. Computational studies of chemical reaction systems have become very popular because the methods are quite reliable and only have medium computational demands compared to *ab initio* molecular orbital theory. In this work, the geometry optimizations of the reactants, products and transition state structures were carried out using Becke's three-parameter density functional [49] and the Lee, Yang, and Parr

functional [50] to describe gradient-corrected correlation effects, which leads to the well-known B3LYP method, combined with two different basis sets. The B3LYP method has been validated to give results similar to that of the more computationally expensive MP2 theory for molecular geometry and frequency calculations [51, 52].

To obtain accurate energies, a complete basis set composite energy method was employed. Traditionally, energy calculations contain only a single computation. To obtain accurate energies, one generally requires a large basis set with a high-level method, which generally takes significant time to compute. Composite energy methods are composed of a series of single point energy calculations steps. Their results are then combined to obtain the highly accurate energy value at a reduced computational cost. The recently developed complete basis set (CBS) methods [53–61] include the basis set truncation errors, the major defect encountered for the single point energy calculations.

In this work, the B3LYP/6-311++g** and B3LYP/aug-cc-pvtz levels of theory [62] were used to calculate geometries and frequencies and compare them in one case with CBS-QB3 [56] energies. This comparing gives us good agreement between the results of our levels of theory with CBS-QB3 results.

We employed the Gaussian 03 program package [63] for our computations. First, all compound's structures were drawn using Gauss View 03 [64] and optimized in semi

Table 1 Selected structures for calculations

Number	Tautomer a	Tautomer b	Number	Tautomer a	Tautomer b
1			5		
2			6		
3			7		
4			8		

empirical PM3 method using Hyperchem 6 program and then Gaussian program to find stationary point geometries characterized as local minimum on the potential energy surface. The absence of imaginary frequencies verified that all structures were true minima at their respective levels of theory.

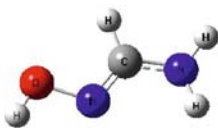



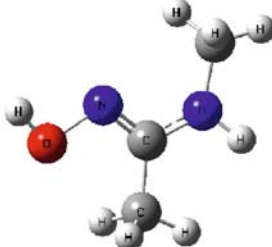
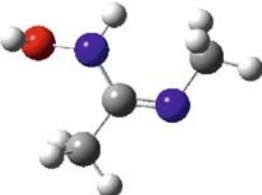
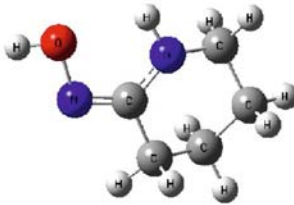
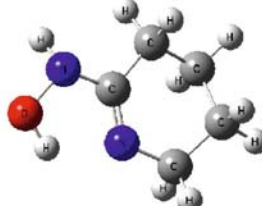
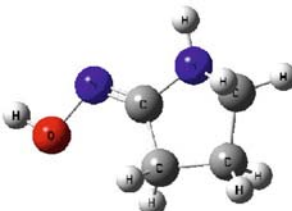



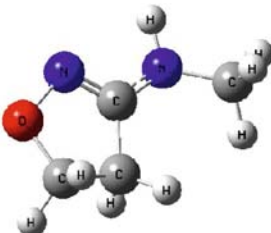
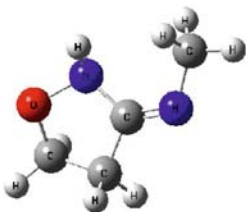


Then, in each pair of compounds, we found and optimized the structure of transition state between them. For each transition state, in traversing from one tautomer to another, stationary point geometry with one imaginary frequency has been found and identified as a transition state by B3LYP methods. To do this, first, we estimated the structure of transition state between two tautomers. Then, its structure was optimized at both B3LYP/6–311++g** and B3LYP/aug-cc-pvtz levels of theory by applying Schlegel's

synchronous-transit-guided quasi-Newton (QST3) method as implemented in Gaussian 03 started from the fully optimized structure of one tautomer and finished on the fully optimized structure of another tautomer.

The products and reactants were verified with frequency calculations to be stable structures, and the transition states were tested to ensure they were first order saddle points with only one negative eigenvalue. Additionally, intrinsic reaction coordinate (IRC) calculations proved that each reaction linked the correct products with reactants.

Solvent effects were studied using an Onsager model in terms of SCRF formalism, by employing the Tomasi's polarized continuum solvation model with PCM variant at B3LYP/aug-cc-pVtZ level. Also acetone (with $\epsilon=20.7$) used as a solvent and United Atom Topological Model

Table 2 Final structure of optimized tautomers

	Tautomer a	Tautomer b		Tautomer a	Tautomer b
1			5		
2			6		
3			7		
4			8		

(UAHF) radii used to build the cavity. The solvation free energies were calculated as the difference between the free energies in solution and gas phase.

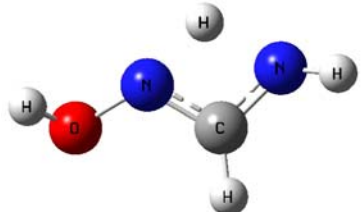
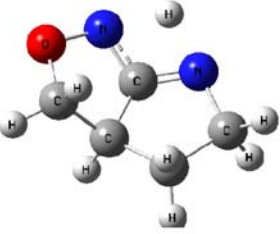
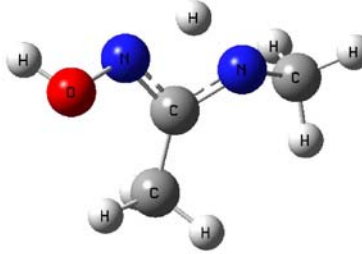
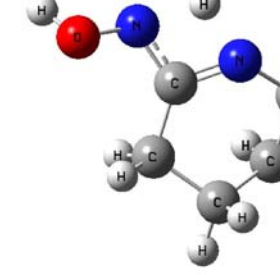
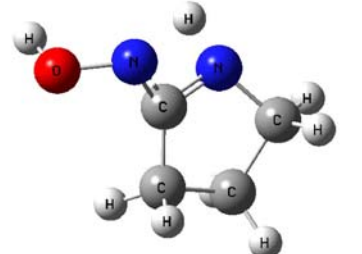
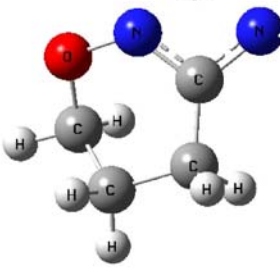
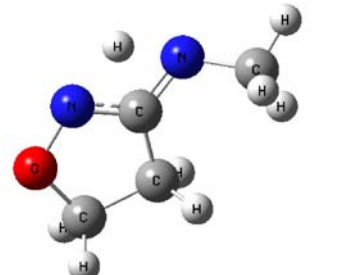
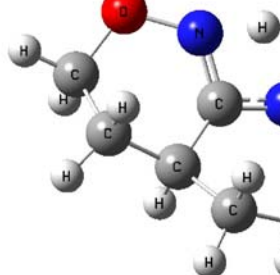
In addition, zero point vibrational energies (ZPVE) were obtained from harmonic vibrational frequencies calculated at the B3LYP method with appropriate scaling factor [65]. All geometries were optimized without any symmetry restrictions and C1 symmetry was assumed for all compounds.

Results and discussion

To begin our research, we have selected eight structures and their tautomers (1a–8a and 1b–8b) from various N-hydroxy amidines. These compounds are shown in Table 1.

The basic structural part of all compounds was numbered as $O_1-N_2(H_5)-C_3-N_4(H_5)$. This part is shared and similar in all tautomers and transition states.

Table 3 Final structure of optimized transition states

T.S. structure	T.S. structure
<p>1</p> 	<p>5</p> 
<p>2</p> 	<p>6</p> 
<p>3</p> 	<p>7</p> 
<p>4</p> 	<p>8</p> 

Optimized structures

The molecular structures of the optimized tautomers are shown in Table 2 and for optimized transition states are shown in Table 3. The calculations of structural parameters are collected in Table 4. All structures extracted from output file of our calculations at B3LYP/aug-cc-pvtz level of theory.

By our fundamental knowledge in organic chemistry, it seems that the first (left) tautomer (tautomer **a** or amide oxime) is more stable than the other tautomer and we are trying to prove this claim by computational method.

Molecular parameters

Two important groups of molecular parameters (bond length and angles) are shown in Table 4. To save space, these parameters have just been shown in shared part of molecules. As expected, CN bond length in tautomer **a** is almost the same as the length of C=N double bond and in tautomer **b** is the same as in C-N single bond. In transition states, this bond length has an amount between single and double CN bond. It shows that through tautomerism, the order of this bond is changed from first order to second order and vice versa. In these tables, the bond length of N-O and OH (if it exists) in all structures are shown. As we expected, there is not any important difference between each of these bond lengths in all structures.

The bond lengths of N₂-H and N₄-H were also reported in the above tables. The amount of this bond is in the range of 0.99–1.02. The difference between these bond lengths is not considerable in all tautomers. However, because of dissociation of this bond through tautomerism, its length is very long in transition states (between 1.3–1.4 angstrom). In addition, it is easily seen that in transition states, the dissociated hydrogen is placed approximately in the middle of two nitrogens and the difference between N₄-H and N₂-H distance is less than 0.18 angstrom.

Observing bond angle variations, we can follow hybridization changes in the central atom of each angle. As an example, N₂-C₃-N₄ bond angle in all tautomers is about 120±3°. It shows the hybridization of central carbon is SP² and it changes rarely in our molecules. This angle in molecule **5a** and **5b** is about 130° that it may be because of tension in the five-membered ring. This angle in transition states is about 105° that is due to the four-membered-like ring in transition states. Viewing the structure of transition states, we find the four-membered-like ring (N₂-C₃-N₄-H₅) that has angles near 90°. It is because of restriction in geometric angles in this ring.

According to Table 4, H₅-N₂-C₃ and H₅-N₄-C₃ angles are in the range of 113 to 120 that their amounts are about hybridational angles of central nitrogen. Certainly, in tautomers **5a** and **5b**, these angles are smaller than the others, which they are about 68–70°. Also in transition

Table 4 Important molecular parameters (bond length in angstrom and angles in degree)

molecule	C ₃ -N ₄	N ₂ -C ₃	O ₁ -N ₂	N ₄ -H	N ₂ -H	O ₁ -H	N ₂ -C ₃ -N ₄	O ₁ -N ₂ -C ₃	C ₃ -N ₄ -H	C ₃ -N ₂ -H
1a	1.38	1.28	1.42	1.01	–	0.96	121.44	110.07	115.08	–
1b	1.27	1.39	1.42	–	1.02	0.96	120.55	112.82	–	112.62
ts1	1.33	1.33	1.42	1.38	1.34	0.96	104.64	116.91	76.62	77.88
2a	1.15	1.29	1.43	1.01	–	0.96	118.24	110.20	114.60	–
2b	1.27	1.41	1.42	–	1.01	0.96	122.73	114.93	–	113.57
ts2	1.33	1.34	1.43	1.37	1.34	0.96	103.25	115.65	77.27	77.89
3a	1.39	1.28	1.43	1.01	–	0.97	121.92	109.37	117.55	–
3b	1.28	1.39	1.42	–	1.02	0.97	121.16	116.05	–	113.14
ts3	1.32	1.33	1.43	1.37	1.37	0.97	105.10	118.73	77.28	76.86
4a	1.38	1.28	1.42	1.01	–	1.44	121.84	108.51	111.58	–
4b	1.27	1.41	1.44	–	1.01	1.44	127.31	108.32	–	116.65
ts4	1.32	1.33	1.45	1.42	1.32	1.44	105.96	108.00	74.70	78.05
5a	1.37	1.28	1.45	1.01	–	1.45	132.65	105.19	119.88	–
5b	1.27	1.39	1.45	–	1.02	1.45	131.28	106.68	–	115.17
ts5	1.30	1.33	1.47	1.38	1.46	1.46	114.19	102.55	73.13	9.69
6a	1.38	1.29	1.44	1.01	–	0.96	124.60	109.81	112.85	–
6b	1.28	1.39	1.41	–	1.01	0.98	117.57	113.84	–	114.22
ts6	1.32	1.34	1.43	1.36	1.36	0.96	103.97	114.79	77.74	76.86
7a	1.70	1.29	1.41	1.01	–	1.43	115.62	118.19	109.73	–
7b	1.27	1.41	1.44	–	1.01	1.43	125.00	115.64	–	114.53
ts7	1.33	1.33	1.42	1.41	1.31	1.43	103.79	120.73	75.84	79.23
8a	1.40	1.29	1.41	1.01	–	1.43	116.70	118.41	110.29	–
8b	1.25	1.41	1.40	–	1.00	1.40	118.78	111.88	–	110.02
ts8	1.33	1.32	1.42	1.45	1.30	1.44	105.62	121.60	74.32	79.85

Table 5 Comparative energetic results of CBS-QB3 with both B3LYP methods (all energies are in kcal mol⁻¹)

Energy entry	cbs	6-311++g**	aug-cc-pvtz	% 6-311++g** error	% aug-cc-pvtz error
ΔE (1a-1b)	8.4	8.0	7.9	5.7	6.5
ΔH (1a-1b)	8.3	8.2	8.1	1.0	1.8
ΔG (1a-1b)	8.4	8.4	8.3	0.3	1.1
$\Delta G^{\#1}$ (TS-1a)	41.3	48.0	48.1	-16.4	-16.6
$\Delta G^{\#2}$ (TS-1b)	32.9	39.6	39.8	-20.6	-21.1

states, this angle is about 68–70° because of four-membered-like ring (N₂-C₃-N₄-H₅). As we considered before, the N₂-C₃-N₄ angle is bigger than the usual amount. Therefore, other angles in four-membered-like ring have to be smaller.

The last important case in the above tables is C₃-N₂-O₁ angle and it is in the range of 110–119°, near the expected angle for SP³ nitrogen.

Kinetic and thermodynamic data

The most important data of our calculations are energies. To examine the accuracy of our DFT calculations (at both 6-311++g** and aug-cc-pvtz levels of theory), we used CBS-QB3 method for obtaining correct energies in the first molecule, its tautomer and their transition state (**1a**, **1b** and TS). In Table 5, the comparative results of this calculation are shown.

From Table 5, it can be seen that both DFT method reproduces the free energy differences between tautomer a and b of each molecule with excellent agreement with both CBS-QB3 method. The percent of error in ΔH and ΔG is less than 2%, so both methods are reliable enough to obtain high accurate energies. Nevertheless, presumably this also

accounts for better accuracy of the B3LYP/6-311++G** computations compared with the B3LYP/aug-cc-pvtz level of theory and the first method gives better results. In addition, from Table 5 it is easily seen that activation energy results of both DFT method are different from CBS method and its percent of error is about 16–21%.

The computed values of ΔG and other thermodynamic parameters at both of these computational levels are presented in Table 6. Also, the energy barrier to conversion of tautomer **a** to **b** and **b** to **a** ($\Delta G^{\#1}$ and $\Delta G^{\#2}$) and corresponded rate constants were computed and shown in this table. All these energies have been calculated in standard condition (298K and one atmosphere). Comparing energies of all tautomers confirms our first estimation about the more stability of tautomer a toward b. The difference between Gibbs free energies in each pair of tautomers is in the range of 4.0–10.2 kcal mol⁻¹ in B3LYP/6-311++G** and 4.4–10.0 kcal mol⁻¹ in B3LYP/aug-cc-pvtz level of theory. It is interesting that this difference in chain molecules is higher than this difference in cyclic molecules. Gibbs free energy difference between transition states and more stable tautomer ($\Delta G^{\#1}$) is in the range of 42.4–71.3 kcal mol⁻¹ and between transition

Table 6 Kinetic and thermodynamic data of all tautomers and transition states, all data in kcal mol⁻¹

B3LYP/6-311++G**								
molecule	$\Delta G^{\#1}$ kcal	$\Delta G^{\#2}$ kcal	k forward	k reverse	ΔE	ΔH	ΔG	Keq
1a,b, ts	48.0	39.6	3.8E-23	5.4E-17	8.0	8.2	8.4	6.9E-07
2a,b, ts	43.5	33.4	7.6E-20	2.2E-12	10.1	9.8	10.2	3.4E-08
3a,b, ts	53.4	43.7	4.3E-27	5.8E-20	9.9	9.8	9.7	7.2E-08
4a,b, ts	52.4	45.1	2.5E-26	5.5E-21	7.4	7.1	7.3	4.4E-06
5a,b, ts	71.3	65.4	3.6E-40	7.4E-36	6.0	5.7	5.9	4.7E-05
6a,b, ts	47.5	38.7	8.9E-23	2.5E-16	9.1	8.7	8.8	3.5E-07
7a,b, ts	42.4	37.6	5.1E-19	1.6E-15	4.7	4.6	4.8	3.1E-04
8a,b, ts	47.3	43.3	1.2E-22	1.1E-19	4.0	4.0	4.0	1.1E-03
B3LYP/Aug-cc-pvtz								
1a,b, ts	48.1	39.8	3.3E-23	4.1E-17	7.9	8.1	8.3	7.9E-07
2a,b, ts	43.6	33.7	6.3E-20	1.3E-12	9.9	9.6	10.0	5.0E-08
3a,b, ts	53.1	43.7	7.4E-27	5.4E-20	9.6	9.5	9.4	1.4E-07
4a,b, ts	68.1	60.8	6.9E-38	1.8E-32	7.5	7.2	7.4	3.9E-06
5a,b, ts	71.1	65.2	4.5E-40	1.1E-35	6.1	5.7	6.0	4.2E-05
6a,b, ts	49.3	41.1	4.5E-24	4.6E-18	8.5	8.1	8.2	9.7E-07
7a,b, ts	42.4	37.4	4.8E-19	2.2E-15	4.9	4.8	5.0	2.2E-04
8a,b, ts	47.4	43.0	1.2E-22	2.0E-19	4.4	4.4	4.4	6.1E-04

Table 7 Solvation effects with kinetic and thermodynamic data in solvent for all molecules at B3LYP/ Aug-cc-pvtz level of theory

molecule	ΔG solvation a	ΔG solvation b	ΔG solvation ts	$\Delta G^{\#1}$	$\Delta G^{\#2}$	k forward	k reverse	ΔG in solvent	Keq in solvent
1a,b, ts	-5.8	-5.5	-4.3	49.7	41.0	2.3E-24	5.1E-18	8.6	4.6E-07
2a,b, ts	-5.0	-5.0	-5.8	42.9	32.9	2.4E-19	4.8E-12	10.0	4.9E-08
3a,b, ts	-6.3	-9.8	-6.3	53.2	47.3	6.6E-27	1.3E-22	5.9	5.1E-05
4a,b, ts	-6.2	-6.3	-6.0	68.4	61.1	4.9E-38	9.9E-33	7.2	5.0E-06
5a,b, ts	-9.8	-7.6	-9.4	71.5	63.3	2.4E-40	2.3E-34	8.2	1.0E-06
6a,b, ts	-7.2	-5.8	-6.4	50.1	40.5	1.2E-24	1.3E-17	9.6	9.7E-08
7a,b, ts	-5.4	-2.6	-5.5	42.3	34.6	5.9E-19	2.9E-13	7.8	2.1E-06
8a,b, ts	-7.2	-5.5	-6.9	47.6	41.5	8.4E-23	2.3E-18	6.1	3.7E-05

states and less stable ($\Delta G^{\#2}$) tautomer is the range of 33.4–65.4 kcal mol⁻¹ in B3LYP/6-311++G** level of theory. Also in B3LYP/aug-cc-pvtz level of theory, the difference between transition states and more stable tautomer ($\Delta G^{\#1}$) is in the range of 42.5–71.7 kcal mol⁻¹ and between transition states and less stable ($\Delta G^{\#2}$) tautomer is in the range of 33.7–65.4 kcal mol⁻¹. The energetic results of both B3LYP calculations are in good agreement with each other.

As well as, the equilibrium constant of tautomerism (obtained from Gibbs free energies) and rate constants of this (obtained from barrier energies) are shown in Table 6. Calculating of rate constants have been carried out in standard methods by Canonical transition state theory [66–69].

From these results, it is easily deduced that the energy difference between tautomers is very low, but the barrier energy of this conversion is so high that the maximum rate constant for this conversion will be $2.2 \times 10^{-12} \text{ s}^{-1}$ at room temperature at both levels. It shows that this conversion is impossible at room temperature.

Finally, we can tell that this conversion can be considered as a kind of 1,3-sigmatropic rearrangement of hydrogen. As we know, such thermal rearrangement for hydrogen is forbidden and our computational result confirms this.

Solvation effect

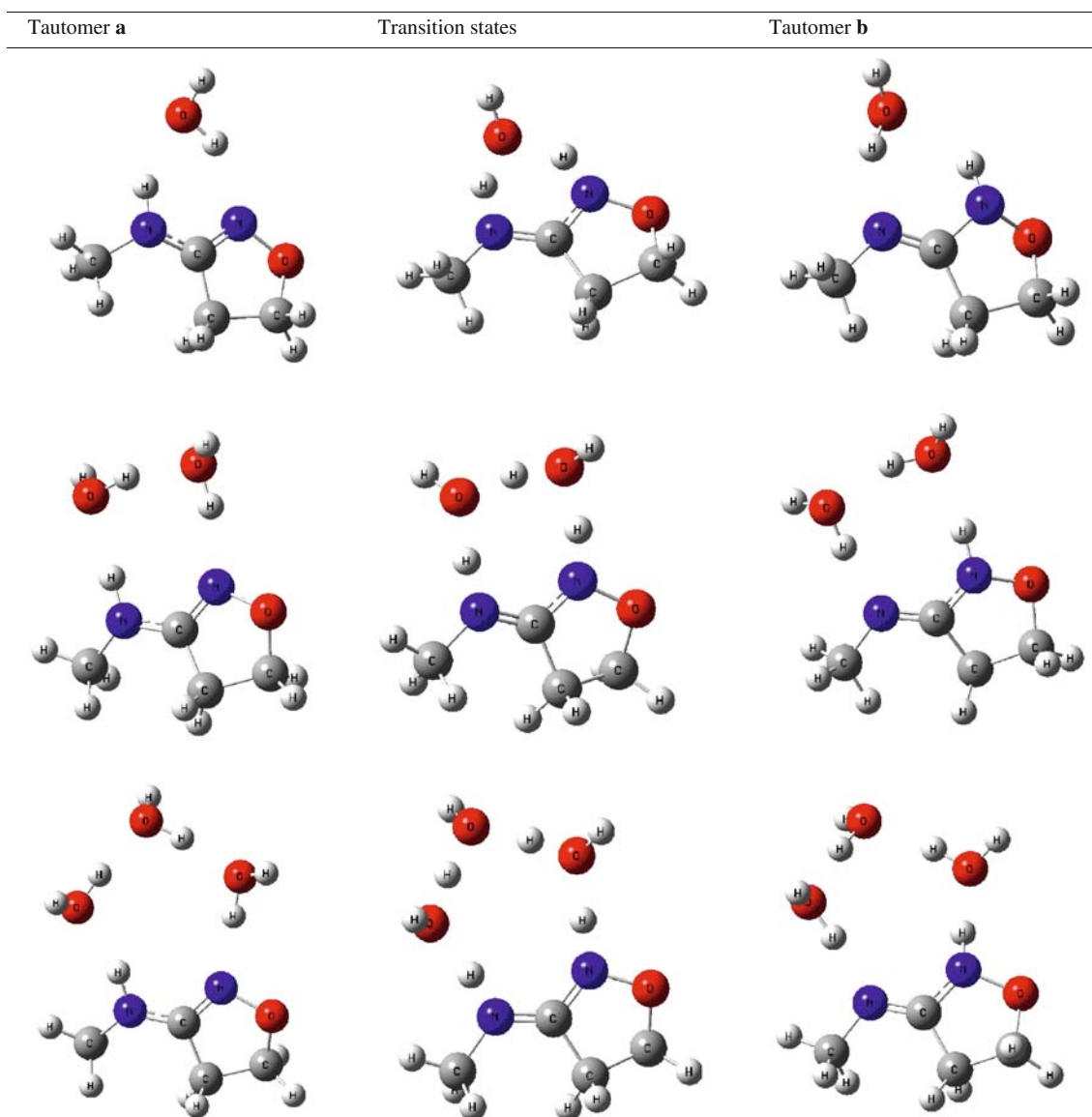
Free energies of hydration were calculated using Tomasi's polarized continuum model (PCM) [70, 71]. The results are presented in Table 7. These calculations provide the total free energy of all molecules in the acetone as a solvent, so the free energy of solvation (in acetone) can be obtained by this method.

As it is shown in Table 7, ΔG solvation for all tautomers and transition states is negative and its amount is in the range of -2.6 to -9.8 kcal mol⁻¹ in all structures. We used these amounts to calculate final ΔG between tautomer in solvent, $\Delta G^{\#}$ between each tautomer and transition state, and finally the rate and equilibrium constants of tautomerism.

Table 8 Most important frequencies of tautomers comparing with reference compounds

	1a	1b	2a	2b	3a	3b	4a	4b
OH	3702.0	3654.9	3705.9	3654.2	3695.8	3548.1	–	–
NH	3527.3	3385.2	348.05	3397.7	3481.6	3389.6	3432.8	3319.9
C=N	1664.4	1640.8	1634.3	1651.9	1673.3	1723.2	1610.8	1681
	Average of computed frequencies				Average of this frequency for Reference compounds*			
OH	3660.2				3373.3			
NH	3427.4				3141.4			
C=N	1660.0				1629.0			
	5a	5b	6a	6b	7a	7b	8a	8b
OH	–	–	3712.8	3331.7	–	–	–	–
NH	3492.5	3389.0	3450.9	3397.9	3414.4	3431.4	3406.4	3658.3
C=N	1657.8	1673.1	1641.4	1648.7	1605.0	1649.9	1604.2	1858.2
	Range of computed frequencies				Range of this frequency for Reference compounds*			
OH	3331–3713				3344–3394			
NH	3319–3658				3022–3235			
C=N	1605–1858				1612–1649			

* references for IR data: ref no. 39 and spectral databases for organic compounds (SDBS no: 5696, 24505,24575)

Table 9 Final structure of optimized tautomers and transition states in presence of 1–3 molecules of water

These data show no important difference between gas phase and solvent media. For example, the maximum rate constant in solvent is $4.8 \cdot 10^{-12} \text{ s}^{-1}$, very near to the gas phase rate constants (minimum: $2.2 \cdot 10^{-12} \text{ s}^{-1}$). In addition, ΔG between each two tautomers in solvent is in the range of 5.9–10.0 kcal mol⁻¹, comparing with the range 4.4–10.0 in the gas phase.

Frequencies

The brief results of corrected IR frequencies are shown in Table 8. To save space, only the most important IR frequencies are reported. These presented frequencies include hydroxy group, imine or oxime C=N double bond and NH bond. Together with these calculated frequencies,

Table 10 Kinetic and thermodynamic data of molecule 4 in presence of 1–3 molecules of water at B3LYP/6-311++G** level of theory

Number of water molecules	$\Delta G^{\#1}$	$\Delta G^{\#2}$	k forward	k reverse	ΔE	ΔH	ΔG	Keq
with one water	20.9	13.6	3.0E-03	7.1E+02	7.2	7.0	7.3	4.2E-06
with two waters	16.7	8.9	3.3E+00	1.9E+06	8.2	7.9	7.8	1.8E-06
with three waters	19.3	10.8	4.5E-02	7.5E+04	8.3	7.9	8.5	6.0E-07
No water, gas phase	52.4	45.1	2.5E-26	5.5E-21	7.4	7.1	7.3	4.4E-06
No water, in solvent	68.4	61.1	4.9E-38	9.9E-33	–	–	7.2	5.0E-06

some experimental frequencies for reported compounds are reported in the above table. Simple comparison of theoretical and experimental frequencies shows the amount of correctness of our frequency calculations.

By observing Table 8, we can see that the frequency of NH bond in transition states is much lower than the same frequency in both tautomers. This is expectable, because this bond cleavages via tautomerism and in the transition state structure, this bond is weaker than in both tautomers.

Water assisted tautomerism

Intermolecular tautomerism of molecule 4 with 1–3 molecules of water is reported in this section. All optimized structures in B3LYP/6–311++G** level of theory are shown in Table 9 and their final kinetic and thermodynamic results comparing with gas phase and solvent data are listed in Table 10.

Viewing these tables, shows us that presence of water molecules near the tautomers and transition state do not have much thermodynamic effect (on ΔG or K_{eq}). As an example, the amounts of ΔG for molecule 4 are 7.29, 7.24 and 7.33 respectively in gas phase, solvent and with one molecule of water. However, surprisingly, complexing of molecule with water make the barrier energy of tautomerism much lower and subsequently the tautomerism rate constant becomes higher. This effect is so intensive that the rate constant for tautomerism of molecule 4a to 4b from $2.48E-26$ in absence of water (in gas phase) goes up to the $2.98E-03$, 3.33 and $4.49E-02$, respectively in the presence of one, two, and three molecules of water. Also this rate constant for converting 4b to 4a from $5.50E-21$ in absence of water (in gas phase) goes up to the $7.09E+02$, $1.85E+06$ and $7.45E+04$, respectively in presence of one, two, and three molecules of water.

At last, we can say although this tautomerism in the absence of water molecule (or each protic media) is very slow or impossible (in gas phase or solvent), in complexing with water molecule, it can be done very fast, especially in the presence of two molecules of water.

Summary

In this work, simple and water assisted tautomerism of some hydroxy amidines were studied using DFT calculations in good agreement with complete basis set composite energy theory. The reactants, products and transition state structures were optimized using the B3LYP/6–311++g** and B3LYP/aug-cc-pvtz levels of theory. In both basis sets used and in all molecules, the tautomer **a** is more stable than tautomer **b**. Then, the structure of transition state between each pair of tautomers was found using QST3 calculation and con-

firmed by FREQ and IRC calculation. From these calculations, barrier energies, rate constants, equilibrium constant and other structural parameters such as IR frequencies, bond length, and angles have been extracted.

The final outcome shows that the barrier energy of this simple tautomerism is very high, but it can be lowered by using water molecules. In the presence of 1–3 molecules of water, this barrier is very low and the rate constant is very high especially in complexing with two molecules of water.

Acknowledgements We are grateful to the Dr. Habibollah Mashhadi and Mr. Mohammad Zakery for their assistance in English editing of our manuscript. In addition, this work has been supported by the research affair of University of Zabol.

References

- Nicolaides DN, Varella EA, in: Patai S (ed), (1992) The Chemistry of Acid Derivatives, vol. 2, Suppl. B, Wiley, New York p875
- Eloy F, Lenaers R (1962) Chem Rev 62:55
- Rehse K, Brehme F (1998) Arch Pharm (Weinheim) 331:375
- Vetrovsky P, Bouche J-L, Schott C, Beranova P, Chalupsky K, Callizot N, Muller B, Entlicher G, Mansuy D, Stoclet J-CJ (2002) Pharmacol Exp Ther 303:823
- Chalupsky K, Lobysheva I, Nepveu F, Gadea I, Beranova P, Entlicher G, Stocklet J-C, Muller B (2004) Biochem Pharm 67:1203
- Oresma L, Kotikoski H, Haukka M, Oksala O, Pohjala E, Vapaatalo H, Moilanen E, Vainiotalo P, Aulaskari P (2006) Eur J Med Chem 41:1073–1079
- Oresma L, Kotikoski H, Haukka M, Oksala O, Pohjala E, Vapaatalo H, Vainiotalo P, Aulaskari P (2006) Bioorg Med Chem Lett 16:2144–2147
- Zhong YL, Zhou H, Gauthier DR, Askin D (2006) Tetrahedron Lett 47:1315–1317
- Yamamoto Y, Tsuritani T, Mase T (2008) Tetrahedron Lett 49:876–878
- Evans MD, Ring J, Schoen A, Bell A, Edwards P, Berthelot D, Nicewongera R, Baldinoia CM (2003) Tetrahedron Lett 44:9337–9341
- Kakanejadifard A, Mahmodi L, Yari A (2006) J Heterocycl Chem 43:1695–1697
- Saeed K, Haider S, Oh T-J, Park S-U (2008) J Membr Sci 322:400–405
- Kavakli PA, Uzun C, Guven O (2004) React Funct Polym 61:245–254
- Caykaraa T, Alaslana SS, Guru M, Bodugoz H, Guven O (2007) Radiat Phys Chem 76:1569–1576
- Zohuriaan-Mehra MJ, Pourjavadi A, Salehi-Radb M (2004) React Funct Polym 61:23–31
- Kitamura A, Hamamoto S, Taniike A, Ohtani Y, Kubota N, Furuyama Y (2004) Radiat Phys Chem 69:171–178
- Farnia SMF, Kakanejadifard A, Soudbar D (1997) Tetrahedron 53:2557–2564
- John K, Gallos JK, Dellios CC (2003) Tetrahedron Lett 44:5679–5681
- Song Y, Clizb L, Bhakta C, Teng W, Wong P, Huang B, Tran K, Sinha U, Park G, Reed A, Scarborough RM, Zhua B-Y (2003) Bioorg Med Chem Lett 13:297–300
- Ghiasvand AR, Ghaderi R, Kakanejadifard A (2004) Talanta 62:287–292

21. Zhang A, Uchiyama G, Asakura T (2005) *React Funct Polym* 63:143–153
22. Nogamia M, Kimb S-Y, Asanuma N, Ikedac Y (2004) *Journal of Alloys and Compounds* 374:269–271
23. Zhang A, Asakura T, Uchiyama G (2003) *React Funct Polym* 57:67–76
24. Choia S-H, Choia M-S, Parka Y-T, Leea K-P, Kang H-D (2003) *Radiat Phys Chem* 67:387–390
25. Shiraishia T, Tamada M, Saitoc K, Sugo T (2003) *Radiat Phys Chem* 66:43–47
26. Sureshbabu VV, Hemantha HP, Naik SA (2008) *Tetrahedron Lett* 49:5133–5136
27. Ferrara M, Crescenzi B, Donghi M, Muraglia E, Nizi E, Pesci S, Summa V, Gardelli C (2007) *Tetrahedron Lett* 48:8379–8382
28. Olaf D, Kinzel OD, Monteagudo E, Muraglia E, Orvieto F, Pescatore G, RicoFerreira MdR, Rowley M, Summa V (2007) *Tetrahedron Lett* 48:6552–6555
29. Ouattara M, Wein S, Calas M, Hoang YV, Viala H, Escaleb R (2007) *Bioorg Med Chem Lett* 17:593–596
30. Oresma L, Kotikoski H, Haukka M, Oksala O, Pohjala E, Vapaatalo H, Vainiotalo P, Aulaskari P (2006) *Bioorg Med Chem Lett* 16:2144–2147
31. Himo F, Lovell T, Hilgraf R, Rostovtsev VV, Noodleman L, Sharpless KB, Fokin VV (2005) *J Am Chem Soc* 127:210–216
32. Durust Y, Akcan M, Martiskainen O, Siirala E, Pihlaja K (2008) *Polyhedron* 27:999–1007
33. Grochowski J, Serda P, Markiewicz M, Kozik B, Sepiol JJ (2004) *J Mol Struct* 689:43–48
34. Kumar A, Jain SK, Rastogi RC (2004) *Theochem* 678:55–61 (b) Enchev V, Abrahams I, Angelova S, Ivanova G (2005) *Theochem* 719:169–175
35. Platonov MO, Samijlenko SP, Sudakov OO, Kondratyuk IV, Hovorun DM (2005) *Spectrochim Acta, Part A* 62:112–114
36. Chung G, Oh HB, Lee D (2005) *Theochem* 730: 241–249 (b) Moreno M, Miller WH (1990) *Chem Phys Lett* 171:475–479
37. Roohi H, Ebrahimi A, Habibi SM (2004) *Theochem* 710: 77–84 (b) Rubin YV, Morozov Y, Venkateswarlu D, Leszczynski J (1998) *J Phys Chem A* 102:2194–2200
38. Foogarasi G, Szalay PG (2002) *Chem Phys Lett* 356:383–390 (b) Yekeler H (2005) *Theochem* 713:201–206
39. Kwiatkowski JS, Leszczynski J (1996) *J Phys Chem* 100:941–953 (b) Ralhan S, Ray NK (2003) *THEOCHEM* 634:83–88
40. Jursic BS (1997) *J Chem Soc Perkin Trans* 2:637
41. Truong TN, Truong TT (1999) *Chem Phys Lett* 314:529
42. Truong TNJ (2000) *Chem Phys* 113:4957
43. Hay PJ, Redondo A, Guo YJ (1999) *Catal Today* 50:517
44. Frash MV, Kazansky VB, Rigby AM, van Santen RA (1998) *J Phys Chem B* 102:2232
45. Bottoni A (1996) *J Chem Soc Perkin Trans* 2:2041
46. Bhan A, Joshi YV, Delgass WN, Thomson KT (2003) *J Phys Chem B* 107:10476
47. Gonzales NO, Chakraborty AK, Bell AT (1998) *Catal Lett* 50:135
48. Rozanska X, van Santen RA, Demuth T, Hutschka F, Hafner J (2003) *J Phys Chem B* 107:1309
49. Becke AD (1993) *J Chem Phys* 98:5648
50. Lee CT, Yang WT, Parr RG (1988) *Phys Rev B* 37:785
51. Johnson BG, Gill PMW, Pople JA (1993) *J Chem Phys* 98:5612
52. Bauschlicher CW, Partridge H (1995) *J Chem Phys* 103:1788
53. Petersson GA, Bennett A, Tensfeldt TG, Allaham MA, Shirley WA, Mantzaris J (1988) *Chem Phys* 89:2193
54. Montgomery JA, Frisch MJ, Ochterski JW, Petersson GA (2000) *J Chem Phys* 112:6532
55. Morihovitis T, Schiesser CH, Skidmore MA (1999) *J Chem Soc Perkin Trans* 2:2041
56. Montgomery JA, Frisch MJ, Ochterski JW, Petersson GA (1999) *J Chem Phys* 110:2822
57. Mayer PM, Parkinson CJ, Smith DM, Radom L (1998) *J Chem Phys* 108:604
58. Ochterski JW, Petersson GA, Montgomery JA (1996) *J Chem Phys* 104:2598
59. Montgomery JA, Ochterski JW, Petersson GA (1994) *J Chem Phys* 101:5900
60. Petersson GA, Allaham MA (1991) *J Chem Phys* 94:6081
61. Petersson GA, Tensfeldt TG, Montgomery JA (1991) *J Chem Phys* 94:6091–6101
62. Lee C, Yang W, Parr RG (1988) *Phys Rev B* 37:785 (1991) 6091
63. Gaussian 03, Revision C02, Frisch MJ et al (2004) Gaussian, Inc, Wallingford CT
64. GaussView, Version 309, Dennington R, Keith T, Millam J, Eppinnett K, Hovell WL, Gilliland R (2003) Semichem, Inc, Shawnee Mission, KS
65. Scott AP, Radom I (1996) *J Phys Chem* 100:16502–16508
66. Masel RI (1996) *Principles of Adsorption and Reaction on Solid Surfaces*. Wiley, New York
67. Masel RI (2001) *Chemical Kinetics and Catalysis*. Wiley-Interscience, New York
68. Holbrook KA, Pilling MJ, Robertson SH (1996) *Unimolecular reactions*. Wiley, New York
69. Gilbert RG, Smith SC (1990) *Theory of unimolecular and recombination reactions*. Blackwell Scientific, Oxford, England
70. Mietrus S, Scrocco E (1981) *J Chem Phys* 55:117
71. Mietrus S, Tomasi E (1981) *J Chem Phys* 65:239